

# Effect of Heat Treatment Conditions on the Electrochemical Capability and Mechanical Properties of Titanium Grade V Alloy for Biomedical Applications

*Onndwela Ramalamula*<sup>1</sup>, *Akinsanya Damilare Baruwa*<sup>1\*</sup> and *Mamookho Elizabeth Makhatha*<sup>1</sup>

<sup>1</sup>Metallurgy Department, University of Johannesburg, Johannesburg, South Africa

**Abstract.** This research aimed to investigate the sustainability of grade V Titanium alloy (Ti-6Al-4V) in NaCl, as well as its mechanical properties for biomedical applications. Improving titanium alloys is critical for producing alloys with minimal side effects. The impacts of structure, indentation test, corrosion resistance, and wear resistance of six titanium alloys after aging were explored in this work. The heat treatment was carried out in a tube furnace with an inert gas, commencing at ambient temperature and progressing to a high temperature of 955°C. For 10 minutes, air and water were used to cool the sample. The samples were then heated to a continuous temperature tempering at 525°C in three steps for both air(A) and water(W) cooled samples 2, 3, and 4 hours. The microstructure was examined using an optical microscope, the corrosion rate was calculated using a potentiostat, hardness was estimated using the Rockwell B scale, and wear resistance was determined using a universal wear tester. It was observed that the water-quenched samples performed better than the air-cooled samples in terms of characteristics. Above all, the dwelling period during the aging process has a greater influence on the material's characteristics.

## 1 Introduction

Titanium and titanium-based alloys have unique qualities such as high strength, low density, and great corrosion resistance; these properties are critical in the production of lightweight and high-strength components for biomedical applications[1,2]. One of the widely recognized Titanium alloys which tend to be utilized in biomedical applications is grade 5 (Ti-6Al-4V, Ti64). Ti-6Al-4V represents an  $\alpha$ - $\beta$  titanium alloy known for its remarkable specific strength and outstanding corrosion resistance. It stands as one of the most commonly employed titanium alloys across a diverse array of applications.

Its popularity stems from its ability to deliver a potent combination of attributes, including low density and superb resistance to corrosion. This makes it an indispensable choice in

---

\* Corresponding authors: [darebaruwa@gmail.com](mailto:darebaruwa@gmail.com)

industries where lightweight materials and exceptional corrosion resilience are paramount, including aerospace and biomechanical engineering[3].

Microstructure plays an important role in the functionality and applications of a material. Microstructure is the determinant factor that forms other properties of the material because the macrostructure influences the mechanical properties; it also influences the corrosion of the material. The microstructure of Ti-6Al-4V includes (alpha)  $\alpha$  -type very tiny acicular needles,  $\alpha + \beta$  lamellar structures, and (beta)  $\beta$ -type grains[4]. Titanium alloy microstructures generally have a lamellar structure of  $\alpha$  and  $\beta$ . However, the morphology may alter due to heat treatment or the amount of  $\beta$  elements added [5]. Much research has been conducted to determine how phase size and organization impact mechanical qualities. The strength of the alloy will rise as the volume percentage of the phase increases, and the qualities will be similar to those of the human body.

Heat treatment can change the microstructure and phase composition of Ti-6Al-4V (Ti64) alloy, affecting its hardness[6]. Ti64's hardness, tensile, and fatigue strength can be increased by annealing at high temperatures [7]. Different heat treatments can produce varying proportions of equiaxed-phase and lamellar microstructures with varying hardness values[8]. Wear resistance is a material's ability to withstand material loss caused by mechanical action [9]. Toughening at 927°C - 1038°C can improve the hardness, tractability, and weakness strength of Ti64, which might further develop its wear resistance. The specific impact of intensity therapy on wear resistance might rely upon the kind, term and temperature of the intensity therapy, as well as the wear system and conditions [10].

Titanium composites have ended up being better as far as biocompatibility due to their fantastic consumption opposition [11]; the expanded utilization of titanium and its compounds as biomaterials comes from its unrivalled biocompatibility and superb erosion obstruction in light of the slight layer of surface oxide and great mechanical properties, for example, a specific modulus of versatility and low thickness that make these metals present a conduct repairman like the bones [12]. One of the biggest negative aspects of using titanium alloy implants is premature failure owing to high wear and corrosion [13]. They add that these frequently result in total revision arthroplasty due to a variety of diagnoses, with higher recurrence of infection, mechanical loosening, fractures, and dislocation. Also, the tribo-corrosion process, which involves sliding corrosion and fretting under body fluids, generates wear debris from the implant, which causes reactions, bone resorption, and low osseointegration of the implant, which may result in a complete revision [14], cytotoxic reactions and neurological problems in the patient [15].

Heat treatment or surface modification may be implemented to improve its characteristics for biochemical applications. The amount and microstructure phases in the alloy will change due to heat treatment. The microstructure will fluctuate greatly depending on the particular heat treatment and manner of processing used[16]. It is expected that its biocompatibility will be enhanced through improvements in corrosion and mechanical properties. This study aims to find out how heat treatment affects the properties of Ti-6Al-4V. Knowing how Ti64 goes through a phase transition during heat treatment and aging can help predict how properties will evolve. In order to achieve the desired biomedical application, the aging parameters will be controlled, resulting in varying microstructure and properties like corrosion rate, wear resistance, and hardness.

## 2 Methodology

### 2.1 Materials

The material under investigation was the  $\alpha+\beta$  Ti-6Al-4V alloy, which was acquired in plate form and complied with the specifications outlined in AMS 4911L [17]. The chemical composition of the initial material is presented in Table 1.

**Table 1:** Chemical composition of as-received Ti-6Al-4V alloy in wt. %

| Element  | Concentration(wt.%) |
|----------|---------------------|
| Aluminum | 6.75                |
| Vanadium | 4.50                |
| Iron     | 0.30                |
| Oxygen   | 0.20                |
| Carbon   | 0.08                |
| Nitrogen | 0.05                |
| Hydrogen | 0.015               |
| Yttrium  | 0.005               |
| Titanium | Balance             |

### 2.2 Heat treatment.

The titanium alloy, denoted as Ti64, underwent a meticulously controlled heat treatment process. To prevent any undesirable oxidation during heating, this treatment was meticulously conducted within a controlled environment utilizing a tube furnace. The material was subjected to a gradual temperature increase, with a heating rate of 10°C per second, starting from an initial temperature of 25°C and progressing up to a temperature of 955°C, which corresponds to a single-phase  $\beta$  region within the alloy's phase diagram. Upon reaching this critical temperature, it was held for a duration of one hour to ensure the complete transformation of the microstructure into the desired  $\beta$  phase.

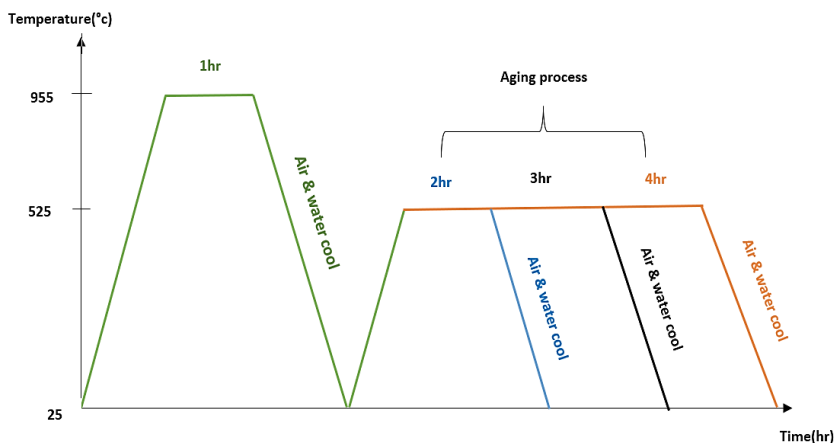


**Fig. 1:** Solution heat treatments and aging treatments of Ti-6Al-4V.

Subsequently, the specimens were subjected to a cooling process, with some being air-cooled while others were rapidly quenched in water. Following this heat treatment phase, the cooled samples entered an aging procedure aimed at enhancing their mechanical strength. This aging process varied in duration, spanning periods of 2, 3, and 4 hours for different specimens. It is worth noting that both air-cooling and water-quenching methods were employed for the aging process. The resulting microstructural changes and property enhancements are represented in Fig. 1, providing a visual depiction of the entire heat treatment process.

## 2.3 Characterization

For accurate characterization, the samples were prepared according to standard AMS 4911L. To characterize the microstructural characteristics,  $\alpha$  and  $\beta$  platelet structure, and optical microscopy was utilized. Corrosion resistance was assessed via electrochemical experiments using potentiodynamic polarization method and sodium chloride solution as the corrosive environment. Mechanical testing and hardness measurements were also done to evaluate the mechanical characteristics of the samples. A Rockwell B scale was used to test the hardness, and a Universal wear testing machine was used.

## 3 Results and Discussion

### 3.1 Microstructure

An optical microscope was employed to examine the distribution of grains, as depicted in Fig. 2. The images were captured at a lower magnification level to determine the presence of phases within the microstructure. Fig. 2b to 2f were attained after the aging process. The as-received shows an equiaxed structure with more of  $\alpha$  phases than  $\beta$  phases. This is because of the amount of Al and V composition within the elementary matrix. The grains are visible, distinct, and the grain boundaries can be easily identified.

Fig. 2b and 2c show slight changes in microstructure, in which both are starting to develop  $\beta$  phases than  $\alpha$  phases. In Fig. 2b, nucleation of  $\beta$  is evident and emanates from the slow cooling of the material as a result of annealing. There are alpha phases protuberance within the structure. However, Fig. 2c displays the Bi-modal type microstructure which is similar to the one reported by Dewangan and Singhal [18]. As the aging time increases the  $\beta$  phases are now dominated more in water-quenched samples than air-cooled samples, as can be seen in Fig. 2e and 2f [19].

It is also worth noting that the  $\alpha$  phases are non-uniform and show that the  $\alpha$  phases (secondary) have different particle sizes. The aging temperature, being slightly below the  $\beta$  temperature, facilitates the attainment of the highest quantity of  $\alpha'$  after the  $\beta$  phase has been quenched in water. Following the aging process at a temperature of 550°C, noteworthy changes in the microstructure became evident. Specifically, the primary  $\alpha$  phase was observed to manifest as smaller islands within the microstructure. These islands coexisted with colonies of both  $\alpha$  and  $\beta$  thin plates, creating a distinctive and complex microstructural arrangement. This transformation represents a significant shift in the material's composition and structure, contributing to altered mechanical properties and behaviour. From Fig. 2, it can be observed that the higher the aging time, the more the disappearance of  $\beta$  phases (more pronounced with water-quenched samples) in the microstructure; this would cause an increase in the strength of the alloy at the detriment of ductility.

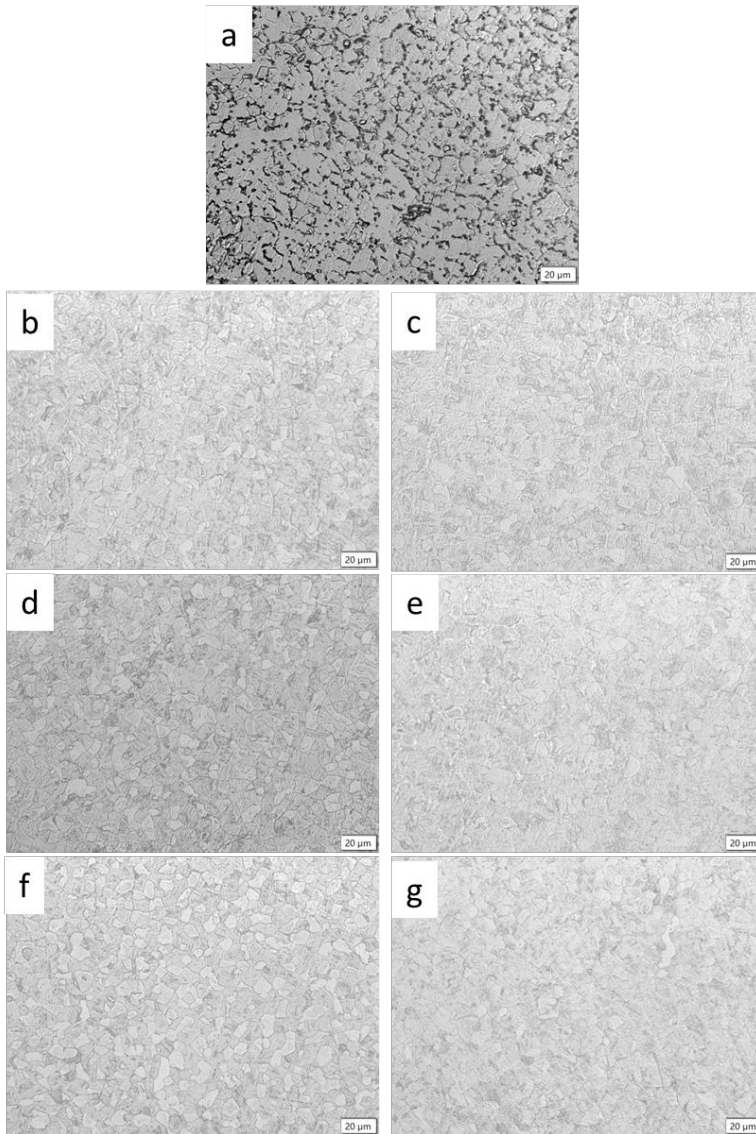


**Fig. 2:** Microstructures of: a) As-received Ti64, b) AC-2hrs, c) WQ-2hrs, d) AC-3hrs, e) WQ-3hrs, f) AC-4hrs, and g) WQ-4hrs, respectively

### 3.2 Mechanical properties

#### 3.2.1 Hardness

Fig. 3 illustrates a comparison of the hardness values of Ti64. The results reveal a significant correlation between the duration of aging in water-quenched materials and the elimination of unstable  $\beta$  phases.

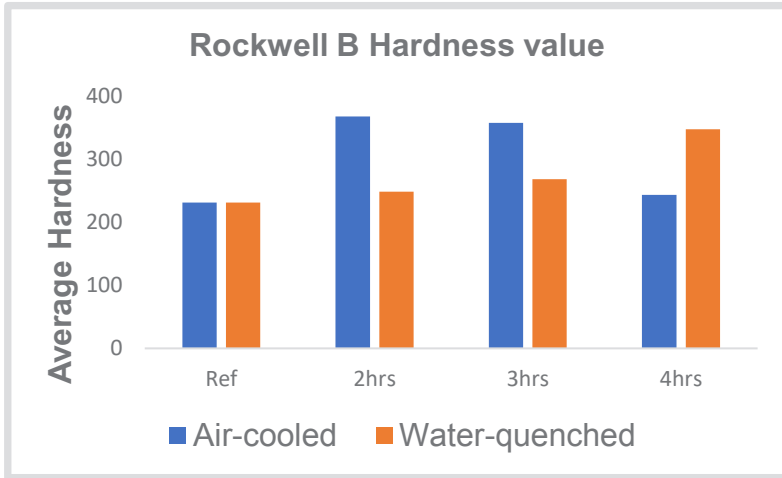


**Fig. 3:** Hardness values of Ti-6Al-4V.

Notably, as the aging period lengthens, there is a pronounced reduction in the presence of these unstable  $\beta$  phases. The sample aged at 4 hrs experienced an improved hardness property. In contrast, when examining air-cooled samples, an increase in aging time is associated with a decrease in hardness values. The sample added for 2 hrs experienced 150 HRB increment in hardness value compared to the reference sample, while the hardness value got reduced over time. Hardness testing indicated a clear progression of hardness as treatment severity increased in the case of the water-quenched samples, indicating the influence of microstructural alterations. It is noteworthy that Yaser et al. [20] have reported a similar trend in hardness values for water-quenched samples, corroborating our findings. The ultimate tensile strength would be increased as treatment time progressed, along with a corresponding reduction in elongation, underscoring the relationship between microstructure, strength, and ductility. This is a result of the unstable  $\beta$  phase, which is relatively soft and ductile in nature [21].

### 3.2.1 Wear resistance

Wear is a critical consideration in numerous engineering applications involving materials subjected to sliding interactions. Understanding wear behaviour, especially in titanium, is essential for optimizing material performance and enhancing component longevity. Equations 1 to 3 were used to investigate wear characteristics in titanium samples under various conditions to establish wear trends and gain insights into wear resistance mechanisms.

$$\text{Wear Volume} = \frac{\pi h}{6} \left[ \frac{3}{4} d^2 + h^2 \right] \tag{1}$$

$$\text{Wear Rate} = \frac{\text{Wear Volume}}{\text{Sliding Distance}} \tag{2}$$

$$\text{Wear Resistance} = \frac{1}{\text{Wear Rate}} \tag{3}$$

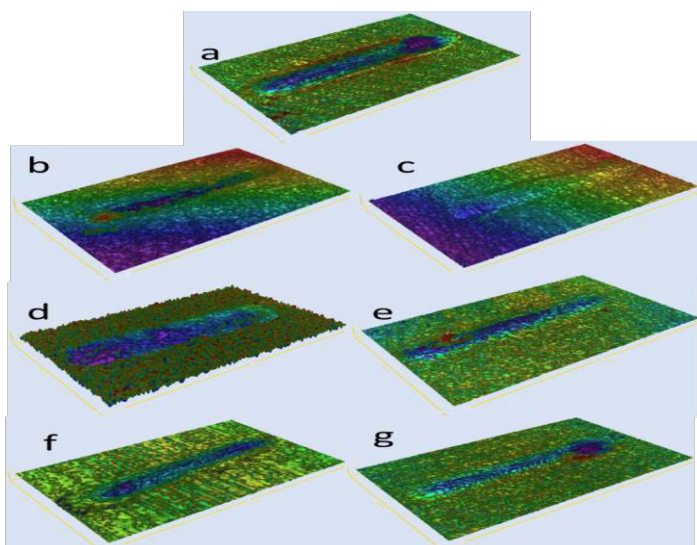
Where  $h$  represents the averaged indentation heights, and  $d$  means averaged wear scar width. These were obtained from the tribometer. The micrograph of the wear mechanism is shown in Fig. 4.

Table 2: The wear characteristics obtained and calculated from the tribometer output

| Sample | dh (µm) | dx (µm) | Sliding Distance (m) | Wear Volume (mm <sup>3</sup> ) | Wear Rate (mm <sup>3</sup> /m) | Wear resistance (m/mm <sup>3</sup> ) |
|--------|---------|---------|----------------------|--------------------------------|--------------------------------|--------------------------------------|
| Ref    | 0.578   | 335.23  | 0.00182              | 2.55E-05                       | 0.01400                        | 071.4086                             |
| AC2    | 0.230   | 227.16  | 0.00163              | 4.66E-06                       | 0.00286                        | 349.6791                             |
| WQ2    | 0.884   | 296.72  | 0.00162              | 3.06E-05                       | 0.01887                        | 052.9976                             |
| AC3    | 1.346   | 354.94  | 0.00169              | 6.66E-05                       | 0.03941                        | 025.3758                             |
| WQ3    | 0.180   | 243.25  | 0.00157              | 4.18E-06                       | 0.00266                        | 375.3351                             |
| AC4    | 0.311   | 279.82  | 0.00168              | 9.55E-06                       | 0.00568                        | 175.9479                             |
| WQ4    | 0.433   | 237.56  | 0.00156              | 9.59E-06                       | 0.00615                        | 162.7289                             |

The amassed data provide valuable insights into the wear characteristics of titanium samples across diverse conditions. These wear volume measurements serve as indicators of the material loss attributed to wear. Notably, samples AC2 and WQ3 stand out with the lowest wear volumes, signifying significantly improved wear resistance, showcasing an 80% and 83% advantage over the remaining samples, respectively. In contrast, samples WQ3 and AC3 exhibit comparatively higher wear volumes, pointing to a greater susceptibility to material loss. Nevertheless, when compared to untreated Ti64, these wear volumes demonstrate a notable reduction.

Wear rates provide information on the rate of material removal over the sliding distance. Sample AC2 and WQ3 exhibited the lowest wear rate, signifying its exceptional wear resistance. Interestingly, samples AC3 and WQ4 displayed relatively higher wear rates despite their lower wear volumes, implying different wear mechanisms for these samples, which could have resulted from the width of the wear track. The wear resistance parameter, defined as the inverse of wear rate, highlights the materials' ability to withstand wear under specific conditions. Sample WQ3 demonstrated the highest wear resistance, showcasing its superior performance under the given sliding conditions. The wear profile in Fig. 4 indicates the wear trends of the untreated and treated Ti-6Al-4V. Through the analysis, Reference, AC3 and WQ2 underwent ploughing action in the counterface as a result of hard asperities [22].



**Fig. 4:** Wear profile of: a) As-received Ti64, b) AC-2hrs, c) WQ-2hrs, d) AC-3hrs, e) WQ-3hrs, f) AC-4hrs, and g) WQ-4hrs, respectively

This indicates a severe plastic deformation on those samples due to excessive wear volume through deeper grooves evident in the samples. Other heat treatment conditions show an adhesive wear mechanism. Other characterizations show a defined pattern except for wear rate.

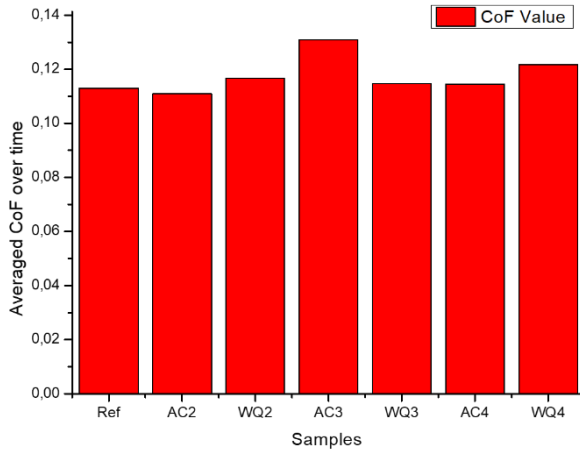


**Fig. 5:** Averaged coefficient of friction of the samples under different conditions

The coefficient of friction was investigated under a normal load of 5 kgf during dry sliding conditions. The average values are depicted in Fig. 5. Along the wear profile data, these values do not exhibit a discernible trend. This suggests the presence of mixed mechanisms and yielding contact areas, resulting in a non-uniform distribution of frictional forces both along and across the wear track junctions.

### 3.3 Corrosion

The obtained results highlight the intricate relationship between cooling methods, aging time, corrosion kinetics, and the propensity for material degradation. This discussion elucidates the nuanced insights drawn from the data in Table 3, providing a profound understanding of how cooling conditions and aging time influence the corrosion resistance of Titanium Grade V. The analysis of corrosion potential ( $E_{corr}$ ) is a pivotal aspect of assessing the likelihood of corrosion initiation. The data obtained from Table 3 shows that water quenching yields more positive  $E_{corr}$  values compared to air cooling. This observation aligns with the widely accepted notion that more negative  $E_{corr}$  values correlate with higher susceptibility to corrosion [23]. The corrosion potential ( $E_{corr}$ ) exhibited fluctuations across different cooling processes. The values ranged from -370.46 mV to -210.74 mV, suggesting varying tendencies toward corrosion initiation. The results suggest that the change from air cooling to water quenching thus enhances the alloy's corrosion resistance. The corrosion rate also corroborates the influence of cooling conditions. The constantly lower  $I_{corr}$  values for water quenching in comparison to air cooling reflect reduced corrosion rates. This trend stresses that more corrosion mitigation is achieved through water quenching, which substantiates its superior protective attributes. Likewise, corrosion current ( $I_{corr}$ ) values demonstrated huge differences between cooling methods. From the data obtained, air cooling for 3 hours yielded the lowest  $I_{corr}$  (0.266  $\mu$ A), indicating superior corrosion resistance, while other cooling processes exhibited comparatively higher  $I_{corr}$  values.

**Table 3:** The electrochemical data from potentiodynamic polarization

| Sample    | $E_{corr}$ (mV) | $I_{corr}$ (uA) | $\beta_c$ (mV) | $\beta_a$ (mV) | Corrosion rate (mmpy) | Efficiency |
|-----------|-----------------|-----------------|----------------|----------------|-----------------------|------------|
| Reference | -370.46         | 8.697           | 524.5          | 222.5          | 0.089957              |            |
| AC2       | -201.35         | 0.388           | 152.6          | 424.2          | 0.004176              | 0.955387   |
| WQ2       | -145.40         | 0.423           | 153.8          | 317.7          | 0.000419              | 0.951363   |
| AC3       | -187.62         | 0.266           | 131.2          | 434.5          | 0.002876              | 0.969415   |
| WQ3       | -248.78         | 5.902           | 717.3          | 126.9          | 0.068166              | 0.321375   |
| AC4       | -177.90         | 0.561           | 177.4          | 423.5          | 0.006228              | 0.935495   |
| WQ4       | -177.91         | 1.169           | 196.6          | 342.8          | 0.001196              | 0.865586   |

The cathodic and anodic slopes of the Tafel plot provide insights into the kinetics of cathodic and anodic reactions. From the general knowledge, elevated Tafel slope values are indicative of accelerated corrosion rates. Remarkably, air cooling yields higher B values, suggesting a more rapid corrosion progression than water quenching. This finding suggests that cooling methods play a pivotal role in modulating the corrosion kinetics of Ti64. These results indicate that the cooling process can influence the activation energies associated with both cathodic and anodic reactions and further affect the material's overall corrosion behaviour. The corrosion rate values underscore the impact of cooling conditions on the degradation rate. The lower corrosion rates observed in water-quenching scenarios, elucidating its potential as an effective strategy for mitigating corrosion-induced material loss. These results suggest the need for careful consideration of cooling techniques in applications requiring prolonged material lifespan. Furthermore, the calculated corrosion rates corroborate the trends observed in the electrochemical parameters. Cooling processes with lower corrosion rates (3 hours water quenching- 0.0004196 mmpy) enhanced corrosion resistance. On the hand, air cooling for 2 hours exhibited the highest corrosion rate (0.089957 mmpy), highlighting its reduced corrosion resistance.

## 4 Conclusions

In conclusion, Ti-6Al-4V is a crucial material in biomedical applications due to its exceptional properties, and therefore, the impact of heat treatment on its properties has been investigated. These observations are hereby drawn:

- 1) The  $\alpha$  and  $\beta$  phases of the microstructure can be altered through heat treatment, impacting its hardness and mechanical properties due to high composition of Vanadium and Aluminium. The higher the duration of heat treatment, the more  $\beta$  phase precipitation in the matrix.
- 2) The more the aging time, the higher the hardness value for the water-quenched while air-cooled increased and diminished in strength after 3 hours of aging. However, the wear resistance and wear rate of both cooling methods were offsetting. There was no cooling method that was distinct.
- 3) The more the aging time, the higher the hardness value for the water-quenched while air-cooled increased and diminished in strength after 3 hours of aging. However, the wear resistance and wear rate of both cooling methods were offsetting. There was no cooling method that was distinct.
- 4) The corrosion potential ( $E_{corr}$ ), corrosion current density ( $I_{corr}$ ) and efficiency revealed variations across different cooling processes.

Overall, this research gave an insights into the influence of heat treatment and cooling methods on the properties of Ti-6Al-4V alloy, providing a foundation for further optimization of these materials for biomedical applications.

## References

1. A. M. Khorasani, M. Goldberg, E. H. Doeven, and G. Littlefair, *J Biomater Tissue Eng* **5**, 593 (2015)
2. F. Li, B. Qi, Y. Zhang, W. Guo, P. Peng, H. Zhang, G. He, D. Zhu, and J. Yan, *Metals (Basel)* **11**, 1 (2021)
3. D. Srinivasan, A. Singh, A. S. Reddy, and K. Chatterjee, *Materials Technology* **37**, 260 (2022)
4. M. S. Baltatu, C. Chiriac-Moruzzi, P. Vizureanu, L. Tóth, and J. Novák, *Applied Sciences (Switzerland)* **12**, (2022)
5. L. Ren, W. Xiao, H. Chang, Y. Zhao, C. Ma, and L. Zhou, *Materials Science and Engineering: A* **711**, 553 (2018)
6. (2011)
7. P. O. Omoniyi, E. T. Akinlabi, and R. M. Mahamood, *IOP Conf Ser Mater Sci Eng* **1107**, 012094 (2021)
8. Y. C. Wang and T. G. Langdon, *J Mater Sci* **48**, 4646 (2013) (n.d.)
9. M. Long and H. J. Rack, *Biomaterials* **18**, 1621 (1998)
10. Q. Chen and G. A. Thouas, *Materials Science and Engineering: R: Reports* **87**, 1 (2015)
11. M. Niinomi, M. Nakai, and J. Hieda, *Acta Biomater* **8**, 3888 (2012)
12. Q. Chen and G. A. Thouas, *Materials Science and Engineering R: Reports* **87**, 1 (2015)
13. P. Nguyen-Tri, T. A. Nguyen, P. Carriere, and C. Ngo Xuan, *International Journal of Corrosion* **2018**, (2018)
14. Z. Paszenda, W. Walke, J. Sonia, Z. Paszenda, W. Walke, and S. Jadacka, *Electrochemical Investigations of Ti6Al4V and Ti6Al7Nb Alloys Used on Implants in Bone Surgery New Ceramic-Polymer Composite for Epithesis with Aluminum-Silicate Microspheres View Project \*\*\* MDPI Crystals Special Issue: "Ceramic Biomaterials Composites Processing"\*\*\*\* View Project Electrochemical Investigations of Ti6Al4V and Ti6Al7Nb Alloys Used on Implants in Bone Surgery* (2010)
15. Z. Y. Zhao, L. Li, P. K. Bai, Y. Jin, L. Y. Wu, J. Li, R. G. Guan, and H. Q. Qu, *Materials* **11**, (2018)
16. R. Gaddam, B. Sefer, R. Pederson, and M. L. Antti, in *IOP Conf Ser Mater Sci Eng* (2013)
17. S. Dewangan and P. Singhal, *Mater Today Proc* **62**, 1570 (2022)
18. P. Yadav and K. K. Saxena, in *Mater Today Proc* (Elsevier Ltd, 2019), pp. 2546–2557
19. Y. Vahidshad and A. H. Khodabakhshi, *Metallography, Microstructure, and Analysis* **11**, 59 (2022)
20. Y. Zhao, M. Lu, Z. Fan, P. McCormick, Q. Tan, N. Mo, and H. Huang, *J Eur Ceram Soc* **40**, 798 (2020)
21. D. Sharma, M. Kamran, N. K. Paraye, and R. Anant, *J Manuf Process* **71**, 669 (2021)
22. B. I. Onyechu, E. E. Oguzie, I. C. Ukaga, D. I. Njoku, and X. Peng, *Portugaliae Electrochimica Acta* **35**, 127 (2017)